Size Control of Semimetal Bismuth Nanoparticles and the UV−Visible and IR Absorption Spectra

Y. W. Wang, Byung Hee Hong, and Kwang S. Kim*

National Creative Research Initiative Center for Superfunctional Materials, Department of Chemistry, Division of Molecular and Life Sciences, Pohang University of Science and Technology, San 31, Hyojadong, Namgu, Pohang 790−784, Korea

Received: August 9, 2004; In Final Form: December 7, 2004

We introduced a simple chemical method to synthesize semimetal bismuth nanoparticles in *N*,*N*-dimethylformamide (DMF) by reducing Bi^{3+} with sodium borohydride ($NaBH_4$) in the presence of poly(vinylpyrroldone) (PVP) at room temperature. The size and dispersibility of Bi nanoparticles can be easily controlled by changing the synthetic conditions such as the molar ratio of PVP to $BiCl_3$ and the concentration of $BiCl_3$. The UV−visible absorption spectra of Bi nanoparticles of different diameters are systematically studied. The surface plasmon peaks broaden with the increasing molar ratio of PVP to $BiCl_3$ as the size of bismuth nanoparticles decreases. Infrared (IR) spectra of the complexes with different molar ratios of PVP/$BiCl_3$ show a strong interaction between the carboxyl oxygen (C═O) of PVP and Bi^{3+} ion and a weak interaction between the carboxyl oxygen (C═O) of PVP and the Bi atom in nanoparticles. This indicates that PVP serves as an effective capping ligand, which prevents the nanoparticles from aggregation.

1. Introduction

Crystalline materials exhibit a variety of interesting optical, electronic, and magnetic features when the physical size of the crystalline approaches to the nanometer scale.[1] Bismuth is a semimetal with a rhombohedral structure. It has a small energy overlap between the conduction and valence bands, high carrier motilities, highly anisotropic Femi surface, and small effective mass. As the crystalline size decreases, the induced semimetal−semiconductor transition would be possible.[2] This size induced semimetal to semiconductor transition and the related quantum confinement effects are potentially useful for optical and electrooptical device applications. Recent work also has suggested that Bi materials of reduced dimensions may exhibit enhanced thermoelectric properties at room temperature.[3]

Most of previous works have focused on either one-dimensional wires fabricated by injecting liquid Bi into the nanochannels of porous anodic alumina membrane or by electrodepositing Bi into templates[4] or on two-dimensional films grown on substrate by using molecular beam epitaxy (MBE).[5] Usually, Bi nanoparticles exhibit quantum confinement effects as their size becomes smaller than the size of electron's wavelength in its bulk solid. Further decrease in size of the nanoparticles causes a semimetal to semiconductor transition. Nevertheless, few studies have been directed toward the Bi nanoparticles so far. Previously, Henglein et al. used the radiolysis reduction of Bi(III) in aqueous solutions to obtain sols of Bi nanoparticles (mean diameter: 20 nm). The absorption spectrum of this colloidal Bi has a weak peak at 253 nm.[6] Recently, Bi nanoparticles were chemically synthesized from the reduction of Bi salts in reverse micelles (water-in-oil inverse microemulsions).[7−9] In these different experiments, the prominent surface plasmon absorption feature was observed at different wavelengths (268 and 280 nm), respectively.[7−9] More recently, using a high-temperature organic solution reduction method, highly crystalline and single domain Bi nanoparticles were synthesized and self-assembled.[10] Buhro et al. also reported the growth of nearly monodispersed Bi, Sn, and In nanoparticles on 1.5 nm Au seeds.[11] However, there is no effective method to control the size and dispersibility of bismuth nanoparticles. Therefore, the dependence of the surface plasmon bands on the size of bismuth nanoparticles has not been successfully observed yet.

In this paper, we introduce a new simple chemical method to synthesize semimetal Bi nanoparticles in *N*,*N*-dimethylformamide (DMF) solution by reduction of Bi^{3+} using sodium borohydride ($NaBH_4$) in the presence of poly(vinylpyrroldone) (PVP). By systematically changing the synthetic conditions such as the molar ratio of PVP to $BiCl_3$ and the concentration of $BiCl_3$, one can easily prepare the high crystalline Bi nanoparticles in narrow size distribution, high dispersibility and single phase purity. More importantly, the diameter of bismuth nanoparticles can be easily controlled from 6 to 13 nm. In particular, we find the gradual broadening of the surface plasmon peak, as the nanoparticle size decreases. We also report infrared spectra (IR) of the pure PVP, the complexes with different molar ratios of PVP/$BiCl_3$, and the Bi nanoparticles capped with PVP molecules. This provides the information on the possible coordination and reaction process for PVP and Bi^{3+} ions (Bi atom). On the basis of these results, we propose the protective mechanism of PVP for the synthesis bismuth nanoparticles.

2. Experimental Section

2.1. Chemicals. $BiCl_3$ was used as precursors of Bi nanoparticles. Sodium borohydride ($NaBH_4$) was used as a reducing agent. *N*,*N*-Dimethylformamide (DMF, 99.9+%, water<0.005%) and poly(vinylpyrroldone) (PVP, M_w = 55 000) were used as solvent and stabilizer, respectively. All of these high grade chemicals were purchased from Aldrich Chemical Company and used without further purification.

* Corresponding author: Tel: +82-54-279-2110, Fax: +82-54-279-8137 Email: kim@postech.ac.kr.

10.1021/jp046423v CCC: $30.25
Published on Web 03/30/2005

2.2. Preparation Procedure of PVP-Protected Bi Nanoparticles. The detailed synthetic procedure of Bi nanoparticles is as follows: 31.5 mg (0.1 mmol) $BiCl_3$ and the designed amount of PVP were dissolved in 10 mL of DMF, which was stirred and degassed using nitrogen for 15 min. The amount of PVP was altered from 0.555 to 55.5 mg (0.005 to 0.5 mmol as a monomeric unit). In addition, 0.3 mL of 1.0 M $NaBH_4$ aqueous solution was injected into 10 mL of DMF and also degassed using nitrogen for 15 min. Then, DMF solution containing $NaBH_4$ was added into the mixture solution of PVP and $BiCl_3$ with constant stirring under flowing nitrogen. Within a few minutes, the colorless solution darkened to black. Stirring was continued for another 5 min after addition. Bismuth nanoparticles were precipitated by adding acetone to the resulting black solution and collected by centrifugation under nitrogen atmosphere. The precipitate was then redispersed into DMF for further characterization.

2.3. Characterization. The disappearance of Bi^{3+} ions and the formation of Bi nanoparticles were confirmed by UV−visible spectra with a HP8453 diode arrays spectrophotometer equipped with a thermostatic multiple sample holder. The bismuth nanoparticle solutions were diluted 30 times with water before taking spectra. Deionized water was used as the reference. The Bi nanoparticles were characterized using energy-dispersed X-ray spectrometry (EDS) as well as high-resolution transition electron microscope (HRTEM JEOL-2010F) operating at 200 kV. To deposit the nanoparticles, the carbon-coated copper grids were dipped directly into colloidal solution, which was previously diluted with ethanol to avoid the dissolution of the polymer layer on the grids by DMF and to decrease the concentration of PVP for better contrast.

IR study was carried out on a Nicolet model 759 Fourier transform infrared spectrometer at wavenumbers 500−4000 cm^{-1} with a resolution of 1 cm^{-1}. The KBr pellets for IR spectra were made by mixing KBr powder with the pure PVP, the complexes and the bismuth nanoparticles capped with PVP molecules. The complexes with different molar ratios of PVP/$BiCl_3$ were prepared by dissolving the corresponding components in methanol. The solution was then cast on a Teflon glass plate and dried in an N_2 environment. The PVP-stabilized bismuth nanoparticles were precipitated by adding acetone to the resulting black solution, and collected by centrifugation under nitrogen atmosphere. The obtained precipitates were washed with a large amount of ethanol, and then dried in an N_2 environment for IR measurement.

3. Results and Discussion

3.1. Formation of Bi Nanoparticles. The formation process of PVP-stabilized Bi (PVP−Bi) nanoparticles ($n_{PVP}/n_{Bi^{3+}} = 0.075$, molar ratio between the monomeric unit of PVP and $BiCl_3$) is described as a representative. Figure 1 shows the UV−visible spectra of PVP, $BiCl_3$ + PVP aqueous solution, and as-prepared bismuth nanoparticle solution diluted with water. Two absorption peaks at 214 and 267 nm are associated with the presence of PVP and Bi^{3+}, respectively. When the addition of $NaBH_4$ into the mixed $BiCl_3$/PVP solution is complete, the peak at 267 nm disappears and a new peak at 281 nm appears. The high optical density at long wavelength is ascribed to the presence of organic solvent (DMF) in the bismuth nanoparticle solutions, which can also be found in the UV-absorption spectra of other metal nanoparticle solutions.[12] The surface plasmon resonance is a characteristic of metal nanoparticles embedded in a dielectric host and is attributed to the collective oscillation of electrons in response to optical excitation. The Bi clusters with diameters below 10 nm did not show any surface plasmon absorption band,[9] while the larger nanoparticles show different absorption peaks at 268 and 280 nm in two different experiments.[7,8] According to calculation,[13] the first absorption band of 10 nm Bi nanoparticles should appear around 270−280 nm. In the present case ($n_{PVP}/n_{Bi^{3+}} = 0.075$, 10 mM $BiCl_3$ solution), the prominent absorption feature at 281 nm is almost certainly the vestige of the plasmon peak characteristics of large bismuth nanoparticles, which is consistent with refs 8 and 10. Therefore, the disappearance of peak at 268 nm and the appearance of a new peak at 281 nm in Figure 1 indicate that the Bi^{3+}ions are reduced completely and the bismuth nanoparticles are formed.

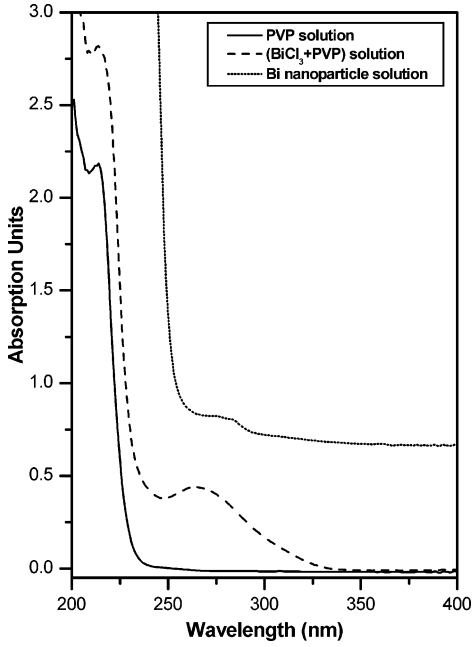

Figure 1. UV−visible spectra of $BiCl_3$ aqueous solution, PVP + $BiCl_3$ aqueous solution and PVP−Bi nanoparticle DMF solution formed with $n_{PVP}/n_{Bi^{3+}} = 0.075$ and 10 mM $BiCl_3$.

The TEM image in Figure 2a further shows the morphology and the size distribution of the as-prepared Bi nanoparticles. This micrograph reveals that the Bi nanoparticles formed in the presence of PVP are spherical. The size of these nanoparticles is in the range of 13 nm in diameter with a broad size distribution. The selected area electron diffraction (SAED) pattern shown in the inset of Figure 2a indicates that the rhombohedral Bi nanoparticles are highly crystalline, which corresponds to the diffraction indices (003), (012), (110), and (013), respectively, according to JCPDS card No. 05-0519.[14] We have further used EDS to address the composition of nanoparticles. The EDS analysis (Figure 2b) demonstrates that the as-prepared nanoparticles contain only Bi element, and no other element is found. The carbon and copper peaks are generated from the carbon-coated copper grid.

3.2. Change of the Absorption Spectra Depending on the Metallic Cluster Size. The absorption spectra of colloidal metal particles depending on the particle size have been reported. If the particle dimensions are smaller than the mean free path of the conduction electrons, collisions of these electrons with the particle surface are noticed.[15] This lowers the effective mean free path.

The theory of the surface plasmon band of metal particles depending on their size was already derived in the past.[16,17] Here, we summarize it in order to facilitate the discussion of our experimental results.

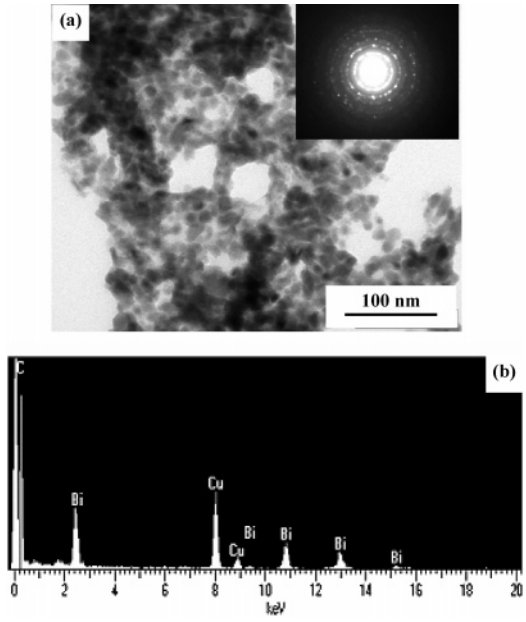

Figure 2. (a) TEM image of the as-prepared Bi nanoparticles ($n_{PVP}/n_{Bi^{3+}} = 0.075$, 10 mM $BiCl_3$). The inset shows the SAED pattern of the as-prepared nanoparticles. (b) EDS pattern of the as-prepared Bi nanoparticles.

In the presence of a dilute colloidal solution containing N particles per unit volume, the measured attenuation of light intensity I_0 over a path length d cm is given by[16]

$$A = \log_{10} I_0/I_d = NC_{ext}d/2.303 \quad (1)$$

where C_{ext} is the extinction cross section of a single particle. In the limit when $2\pi R < \lambda$ (where R is the radius of the particles and λ is the wavelength of the light in the media), only the electric dipole term, developed in Mie's theory, is significant. Then the extinction cross section C_{ext} can be expressed as

$$C_{ext} = \frac{24\pi^2 R^3 \epsilon^{3/2}}{\lambda} \frac{\epsilon_2}{(\epsilon_1 + 2\epsilon)^2 + \epsilon_2^2} \quad (2)$$

where ϵ is the dielectric permittivity:

$$\epsilon = \epsilon_1 + i\epsilon_2 \quad (3)$$

In the case of many metals, the region of absorption up to the bulk plasma frequency is dominated by the free electron behavior, and the dielectric response is well described by the simple Drude model. According to this theory,[17] the real and imaginary parts of the dielectric function are

$$\epsilon_1 = \epsilon^\infty - \omega_p^2/(\omega^2 + \omega_d^2) \quad (4)$$

$$\epsilon_2 = \omega_p^2 \omega_d/\omega(\omega^2 + \omega_d^2) \quad (5)$$

where ϵ^∞ is the high-frequency dielectric constant due to interband and core transitions and ω_p is the bulk plasma frequency

$$\omega_p^2 = Ne^2/m\epsilon_0 \quad (6)$$

in terms of the concentration of free electrons in metal (N), and the effective mass of the electron (m). ω_d is the relaxation or damping frequency, which is related to the mean free path of the conduction electrons (R_{bulk}) and the velocity of electrons at the Fermi energy (v_f):

$$\omega_d = v_f/R_{bulk} \quad (7)$$

When the particle radius (R) is smaller than the mean free path in the bulk metal, the conduction electrons are additionally scattered by the surface, and the mean fee path (R_{eff}) becomes size dependent,

$$1/R_{eff} = 1/R + 1/R_{bulk} \quad (8)$$

The most important parameter affecting ω_d is the particle size. From eqs 2, 7, and 8, it can be seen that a decrease in particle size leads to an increase in ω_d, causing the band to broaden and the maximum intensity to decrease. The position of the peak is virtually unaffected by small changes, while a slow shift to the lower energy occurs for large damping.

3.3. Size Control of Bi Nanoparticles by Varying the Amount of PVP and the Change in UV—Visible Absorption Spectra. The protective polymer, PVP, was widely used as a stabilizer to prevent nanoparticles from aggregation in chemical preparation of noble metal nanoparticles including gold,[18] silver,[19] palladium,[20] and platinum.[21] In this paper, we also used PVP as a stabilizer to prevent Bi nanoparticles from aggregation, as we did to make antimony nanoparticles and nanowires.[22] When the PVP was absent in our synthetic process, black precipitate appeared quickly upon adding the reducing agent solution. However, when very low concentration of PVP was added into the $BiCl_3$ solution, a black nanoparticle solution was obtained after the reaction finished. Furthermore, as more PVP was added, more stable Bi nanoparticle solution was obtained. It is apparent that the PVP keeps the Bi nanoparticles from aggregation during the reaction process. To investigate the protective mechanism of PVP for the synthesis of bismuth nanoparticles, we recorded the IR spectra of the pure PVP, the complexes with different molar ratios of PVP/$BiCl_3$, and the resulting PVP-stabilized bismuth nanoparticles. Parts a−d of Figure 3 show the IR spectra of PVP (Figure 3a) and the PVP/$BiCl_3$ complexes with different PVP/$BiCl_3$ molar ratios of 10 (Figure 3b), 5 (Figure 3c), and 1 (Figure 3d), respectively. The free C═O stretching band of pure PVP is at 1675 cm^{-1}.[23] The intensity of this band diminishes because the number of free C═O band decreases, and a new band at 1588 cm^{-1} appears with the decreasing molar ratio of PVP/$BiCl_3$.[24] This new band is thought to be associated with the coordination interactions between bismuth ions and carbonyl oxygen. The shift of the free C═O band to a lower wavenumber originates from the loosening of the C═O double bond by Bi^{3+}-coordination. When the molar ratio of PVP/$BiCl_3$ increases at a constant concentration of $BiCl_3$, the number of bismuth ions becomes much smaller than the number of carbonyl oxygens in PVP.[25] After reduction of bismuth ions, the number of bismuth atoms present at close range decreases, and so the average size of the bismuth nanoparticles decreases. Furthermore, the IR spectra of the complex with a PVP/$BiCl_3$ molar ratio of 5 and the resulting washed PVP-stabilized bismuth nanoparticles are compared in Figure 4, parts a−c. The disappearances of the bands at 1558 and 1675 cm^{-1} in the IR spectra of PVP-stabilized bismuth nanoparticles are attributed to the reduction of bismuth ions and the removal of free PVP, respectively. A new band at 1659 cm^{-1} appears which is thought to be associated with the weak interactions between the reduced bismuth atoms and the carbonyl oxygen atoms. As Bi^{3+} binds the O atom in the C═O bond, this C═O bond weakens, and the frequency red-shifts by a large amount, while as the reduced Bi atom binds the O atom in the C═O bond, this C═O bond weakens only slightly, and the frequency red-shifts by a small amount. Therefore, the protective

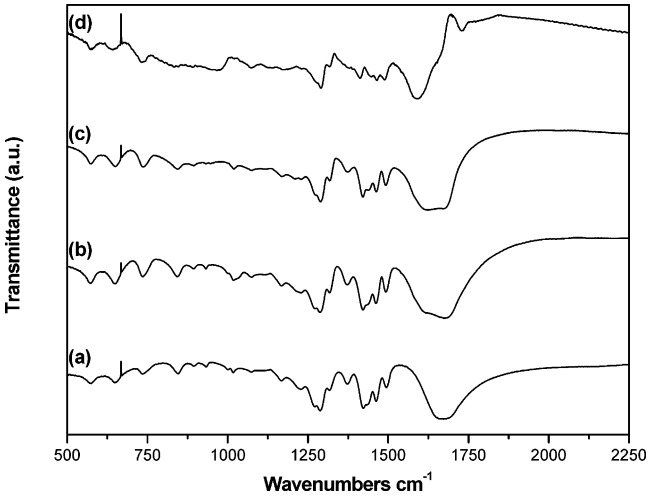

Figure 3. IR spectra of (a) pure PVP; the complexes with different molar ratios of PVP to $BiCl_3$: (b) 10, (c) 5, and (d) 1. In all cases, the concentration of $BiCl_3$ is 10 mM.

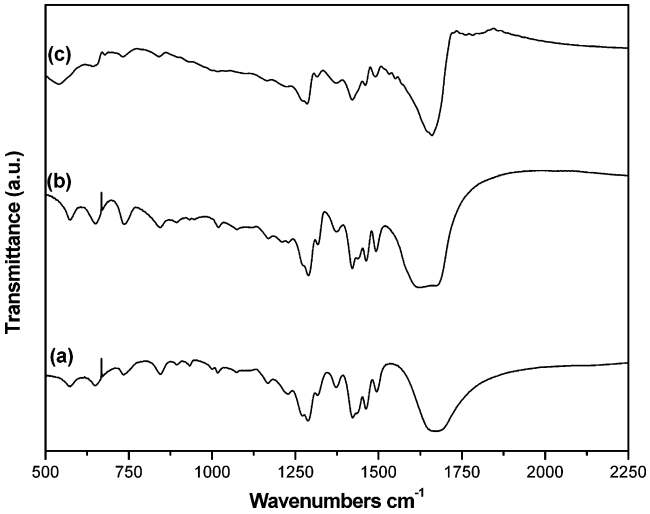

Figure 4. IR spectra of the pure PVP (a), the complex with a PVP/$BiCl_3$ molar ratio of 5 (b), and the resulting bismuth nanoparticles with a PVP/$BiCl_3$ molar ratio of 5 (c).

mechanism of PVP for the synthesis of bismuth nanoparticles is summarized as follows. When PVP and $BiCl_3$ are dissolved in DMF, bismuth ions interact with the carbonyl oxygen of PVP to form the coordinative bonding. Then bismuth ions are reduced to bismuth atoms by adding reducing reagents; subsequently, the nearby bismuth atoms aggregate at close range (increasing the amount of PVP or decreasing the concentration of $BiCl_3$ will result in decreasing the number of bismuth atoms at close range, so the average size of the bismuth nanoparticles decreases). Finally, the PVP adsorbed on the surface of bismuth nanoparticle prevents them from aggregation.

Accordingly, the amount of PVP added to the solution is expected to affect the growth process for the Bi nanoparticles. Therefore, the change in size of the Bi nanoparticles will be investigated by varying the amount of PVP. In the first set of experiments, the concentration of $BiCl_3$ was kept at 10 mM and the concentration of PVP was varied by changing the molar ratios of $n_{PVP}/n_{Bi^{3+}}$ (0.05, 0.10, 0.15, 1.00, 5.00). The UV−visible absorption spectra of these prepared Bi nanoparticle solutions with different molar ratios were also studied, along with the dependence of the surface plasmon absorption band of bismuth nanoparticles on their size.

Figure 5a shows the UV−visible absorption spectra taken from the Bi nanoparticle solutions with different molar ratios between the monomeric unit of PVP and $BiCl_3$. In the case of a molar ratio of 0.15, a continuous absorption spectrum with a shoulder at 281 nm was observed. As the amount of PVP decreases, the absorption peak at 281 nm appears progressively in the absorption spectra. When the molar ratio decreases to 0.05, the prominent surface plasmon absorption peak of Bi nanoparticles at 281 nm is obvious. When the molar ratio increases (from 0.15 to 1.00 and then to 5.00), the shoulder at 281 nm broadens in the absorption spectra, as shown in Figure 5b. Thus, it can be concluded that the surface plasmon absorption peak of Bi nanoparticles gradually broadens with increasing molar ratio of PVP to $BiCl_3$, and then the peak broadens almost completely at a high molar ratio (5.00).

Figure 6 presents the TEM images of the PVP−Bi nanoparticles synthesized with different molar ratios of $n_{PVP}/n_{Bi^{3+}}$ in DMF. Decreasing the molar ratio results in large Bi nanoparticles with a wide range of size distribution. Parts a and b of Figure 6 show the low and high magnification TEM images of a sample synthesized by using the procedure similar to the standard synthesis shown in Figures 1 and 2, except that the molar ratio of PVP to $BiCl_3$ increased from 0.075 to 0.15. In this case, Bi nanoparticles with the average diameter of 11 nm were obtained. Although the average diameter of these Bi nanoparticles just slightly decreased than that obtained at low molar ratio of PVP to $BiCl_3$ ($n_{PVP}/n_{Bi^{3+}} = 0.075$, as shown in Figure 2a), the distribution of diameters and the dispersibility of nanoparticles are better than those in Figure 2a. Increasing the molar ratio of PVP to $BiCl_3$ from 0.15 to 1.00, as shown in Figure 6, parts c and d, the average size of synthesized nanoparticles decreases to ~8 nm. Further increasing the molar ratio from 1.00 to 5.00, the average nanoparticle size decreases down to ~6 nm. In addition, it is easy to find that Bi nanoparticles in Figure 6, parts e and f, are almost isolated and well dispersed, which indicates that the diameter distribution and the dispersibility of these Bi nanoparticles are much better than those synthesized at a low ratio of PVP to $BiCl_3$ shown in Figures 2a and 6a−d. In conclusion, the molar ratio of PVP to $BiCl_3$ is intrinsically important to control the size of the Bi nanoparticles. The Bi nanoparticles with small diameter, high dispersibility, and narrow diameter distribution can be easily obtained by increasing the molar ratio of PVP to $BiCl_3$.

Meier et al.[26] have reported that the plasmon would be suppressed by the finite size effect, as the size of metal particles is very small. By decreasing the gold crystallite size, the absorption spectra show a systematic evolution, specifically, a broadening of surface plasmon band until the crystallites having less than 2.0 nm in effective diameter are unidentifiable.[27] A representative UV−visible spectrum of gold nanoparticles with diameters below 2 nm shows no significant surface plasmon band at 520 nm.[28] Pileni et al.[12] also have proven that a gradual disappearance in the 570 nm plasmon peak occurs upon decreasing the size of the copper clusters. It is clear that the copper particles with a diameter below 4 nm are characterized by a large broadening of the plasmon resonance. In the above-mentioned references, the gradual broadening in the surface plasmon band occurs upon decreasing the size of the metal nanoparticles. This demonstrates experimentally the theory summarized in section 3.2 of this paper. In this study, we also find that the surface plasmon band at the 281 nm gradually broadens as the size of the bismuth nanoparticles decreases. This plasmon band widely broadens when the Bi nanoparticle diameter decrease to 6 nm which is confirmed by TEM images shown in Figure 6. It can be concluded that the surface plasmon band of bismuth nanoparticles gradually broadens with the

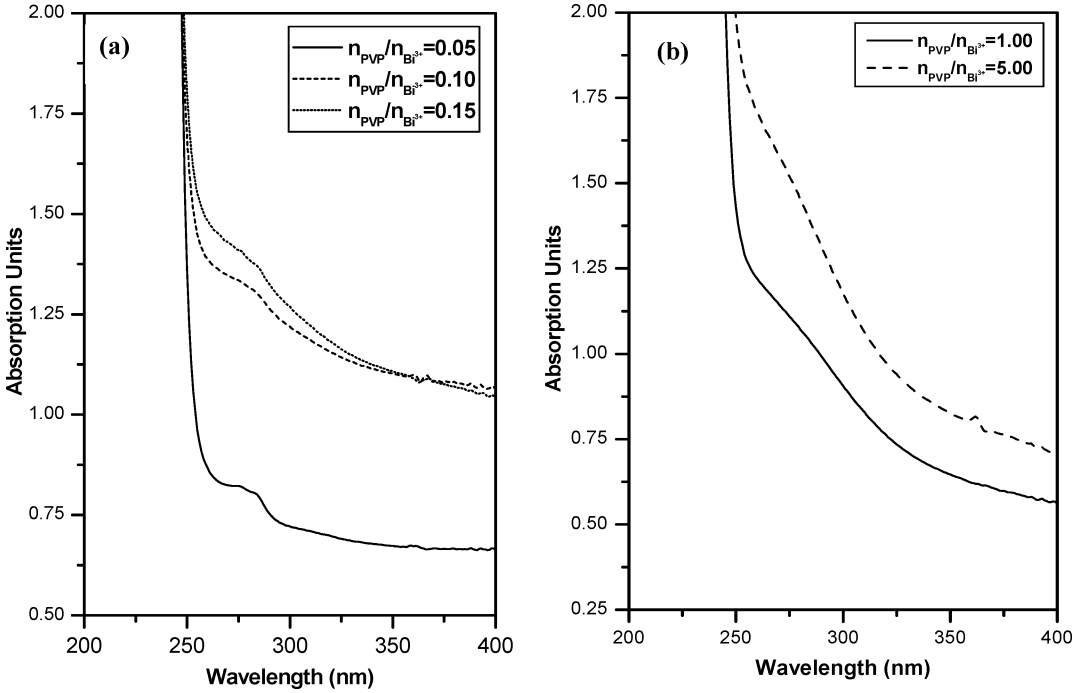

Figure 5. UV−visible spectra of PVP−Bi nanoparticles synthesized at various molar ratios of PVP to $BiCl_3$, keeping the concentration of $BiCl_3$ at a constant value of 10 mM. (a) $n_{PVP}/n_{Bi^{3+}} = 0.05$, 0.075, 0.10, 0.125 and 0.15; (b) $n_{PVP}/n_{Bi^{3+}} = 0.15$, 1.00 and 5.00.

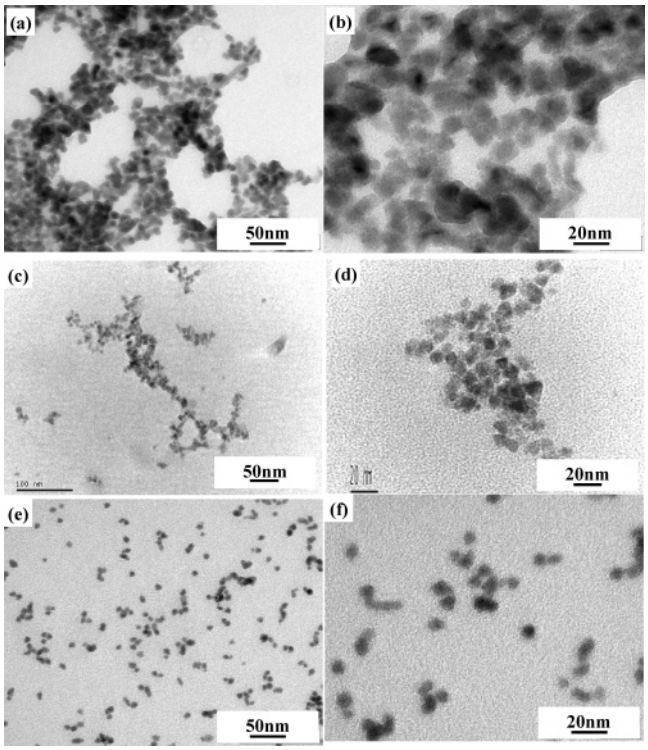

Figure 6. TEM images of PVP−Bi nanoparticles synthesized at various molar ratios of PVP to $BiCl_3$, keeping the concentration of $BiCl_3$ at a constant value of 10 mM. Low and high magnification of the synthesized nanoparticles [(a, b) $n_{PVP}/n_{Bi^{3+}} = 0.15$; (c, d) $n_{PVP}/n_{Bi^{3+}} = 1.00$; (e, f) $n_{PVP}/n_{Bi^{3+}} = 5.00$).

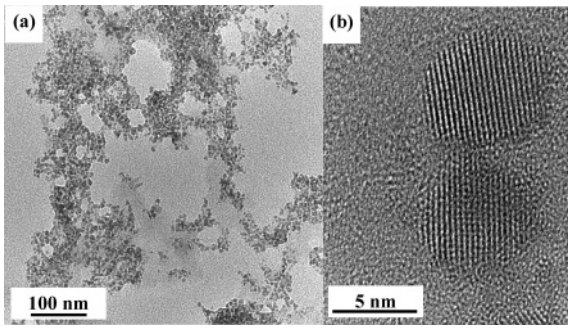

Figure 7. (a) TEM image of PVP−Bi nanoparticles ($n_{PVP}/n_{Bi^{3+}} = 0.075$, 1 mM $BiCl_3$); (b) HRTEM image of the isolated Bi nanoparticles shown in part a.

decreasing nanoparticle size. According to the above analysis, the absence of plasmon band of bismuth clusters in ref 9 is due to the small size of the clusters.

3.4. Size Control of Bi Nanoparticles by Varying the Concentration of $BiCl_3$. The concentration of $BiCl_3$ was also found to play an important role in determining the size of Bi nanoparticles. Figure 7a shows the TEM image of Bi nanoparticles synthesized with 1 mM $BiCl_3$ and 0.075 mM PVP. It can be seen that the Bi nanoparticles with very small diameter of about 6.5 nm are near regular spherical, but the dispersibility is not good because of the low concentration of PVP. The HRTEM image of two isolated nanoparticles is shown in Figure 7b, which provides further insight into the structure of Bi nanoparticles. Dislocations and stacking faults are rarely observed in the HRTEM image. The spacing of the lattice fringes is found to be about 0.32 nm, which indexes to the (012) spacing of rhombohedral Bi. Compared with the product shown in Figure 2a and Figure 5, we can conclude that the decrease in concentration of $BiCl_3$ helps the formation of smaller Bi nanoparticles. When the concentration of $BiCl_3$ decreases with a constant molar ratio of PVP/$BiCl_3$, the number of bismuth ions that can interact with the carbonyl oxygen of a molecule of PVP decreases. After reduction of bismuth ions, the number of bismuth ions present at close range decreases, so the average size of the bismuth nanoparticles decreases.

Figure 8 shows the UV−visible absorption spectra taken from the Bi nanoparticle solutions at different $BiCl_3$ concentrations, while keeping the molar ratio of PVP to $BiCl_3$ at a constant value of 0.075. In the case of a $BiCl_3$ concentration of 10 mM, an obvious surface plasmon absorption peak at 281 nm is

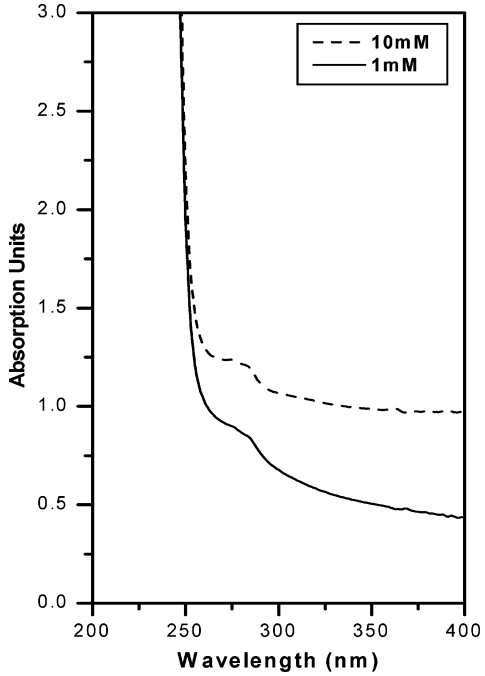

Figure 8. UV−visible spectrum of the as-prepared Bi nanoparticles at different concentrations of $BiCl_3$, keeping the PVP to $BiCl_3$ molar ratio at a constant value of 0.075.

observed. By decreasing the concentration of $BiCl_3$ to 1 mM, the prominent surface plasmon absorption peak broadens, which is due to the decreased size of synthesized Bi nanoparticles. This result is similar to that shown in Figure 5.

4. Conclusion

In this paper, we introduced the method to control the size of Bi nanoparticles in the range 6−13 nm by adjusting the molar ratio of PVP to $BiCl_3$ or the concentration of $BiCl_3$. Well-dispersed small Bi nanoparticles (about 6 nm) with a narrow size distribution were easily synthesized through this method at $n_{PVP}/n_{Bi^{3+}} = 5.00$ and 10 mM $BiCl_3$. It was found that the surface plasmon absorption peak in UV−visible spectra broadened, due to the decreased size of synthesized Bi nanoparticles. The IR study of the pure PVP, the complexes with different molar ratios of PVP/$BiCl_3$, and the PVP-stabilized bismuth nanoparticles demonstrates the protective mechanism of PVP for the synthesis of bismuth nanoparticles.

Compared to Bi nanoparticles synthesized by using other methods, the present nanoparticles show high crystallinity, small diameter, narrow size distribution, high dispersibility, and single phase purity. This synthetic method provides a convenient route for the formation of highly crystalline Bi nanoparticles, which can serve as the basis for further study of quantum-confinement phenomena of small Bi nanoparticles.

Acknowledgment. This work was supported by BK21 and KOSEF/CRI.

References and Notes

(1) (a) Campbell, C. T.; Parker, S. C.; Starr, D. E. *Science*, **2002**, *298*, 811. (b) Tang, Z. Y.; Kotov, N. A.; Giersig, M. *Science*, **2002**, *297*, 237. (c) Volokitin, Y.; Sinzig, J.; deJongh, L. J.; Schmid, G.; Vargaftik, M. N.; Moiseev, I. I. *Nature (London)* **1996**, *384*, 621. (d) Hong, B. H.; Bae, S. C.; Lee, C.-W.; Jeong, S.; Kim, K. S. *Science* **2001**, *294*, 348. (e) Suh, S. B.; Hong, B. H.; Tarakeshwar, P.; Youn, S. J.; Jeong, S.; Kim, K. S. *Phys. Rev. B* **2003**, *67*, 241402(R).

(2) (a) Costa-Kramer, J. L.; Garcia, N.; Olin, H. *Phys. Rev. Lett.* **1997**, *78*, 4990. (b) Liu, K.; Chien, C. L.; Searson, P. C.; Kui, Y. Z. *Appl. Phys. Lett.* **1998**, *73*, 1436. (c) Black, M. R.; Lin, Y. M.; Cronin, S. B.; Rabin, O.; Dresselhaus, M. S. *Phys. Rev. B*, **2002**, *65*, 195417. (d) Black, M. R.; Hagelstein, P. L.; Cronin, S. B.; Lin, Y. M.; Dresselhaus, M. S. *Phys. Rev. B* **2003**, *68*, 235417.

(3) (a) Heremans, J.; Thrush, C. M. *Phys. Rev. B* **1999**, *59*, 12579. (b) Dresselhaus, M. S.; Lin, Y. M.; Rabin, O.; Dresselhaus, G. *Microscale Thermophys. Eng.* **2003**, *7*, 20.

(4) (a) Cheng, Y. T.; Weiner, A. M.; Wong, C. A.; Balogh, M. P.; Lukitsch, M. J. *Appl. Phys. Lett.* **2002**, *81*, 3248. (b) Huber, T. E.; Celestine, K.; Graf, M. J. *Phys. Rev. B* **2003**, *67*, 245317.

(5) (a) Hoffman, C. A.; Meyer, J. R.; Bartoli, F. J.; Divenere, A.; Yi, X. J.; Hou, C. L.; Wang, H. C.; Ketterson, J. B.; Wong, G. K. *Phys. Rev. B* **1993**, *48*, 11431. (b) Hoffman, C. A.; Meyer, J. R.; Bartoli, F. J.; Divenere, A.; Yi, X. J.; Hou, C. L.; Wang, H. C.; Ketterson, J. B.; Wong, G. K. *Phys. Rev. B*, **1995**, *51*, 5535.

(6) Gutierrez, M.; Henglein, A. *J. Phys. Chem.* **1996**, *100*, 7656.

(7) (a) Fang, J. Y.; Stokes, K. L.; Wiemann, J. A.; Zhou, L.; Dai, J. B.; Chen, F.; O'Connor, C. J. *Mater. Sci. Eng. B* **2001**, *83*, 254. (b) Zhao, Y. B.; Zhang, Z. J.; Dang, H. X. *Mater. Lett.* **2004**, *58*, 790.

(8) Stokes, K. L.; Fang, J. Y.; O'Connor, C. J. *18th International Conference on Thermoelectrics*; 1999; pp 374−377.

(9) Foos, E. E.; Stroud, R. M.; Berry, A. D.; Snow, A. W.; Armistead, J. P. *J. Am. Chem. Soc.* **2000**, *122*, 7114.

(10) Fang, J. Y.; Stokes, K. L.; Zhou, W. L.; Wang, W. D.; Lin, J. *Chem. Commun.* **2001**, *18*, 1872.

(11) Yu, H.; Gibbons, P. C.; Kelton, K. F.; Buhro, W. E. *J. Am. Chem. Soc.* **2001**, *123*, 9198.

(12) (a) Lisiecki, L.; Pileni, M. P. *J. Am. Chem. Soc.* **1993**, *115*, 3887. Sun, Y. G.; Yin, Y. D.; Mayers, B. T.; Herricks, T.; Xia, Y. N. *Chem. Mater.* **2002**, *14*, 4736.

(13) Creighton, J. A.; Desmond, G. E. *J. Chem. Soc. Faraday Trans.* **1991**, *87*, 3881.

(14) International Center for Diffraction Data (ICDD), Newtown Square, PA, Powder Diffraction File, Formerly JCPDS.

(15) (a) Wokaun, A.; Gordon, J. P.; Liao, P. F. *Phys. Rev. Lett.* **1982**, *48*, 957. (b) Meier, M.; Wokaun, A. *Opt. Lett.* **1983**, *8*, 581. (c) Euler, J. Z. *Phys.* **1954**, *137*, 318.

(16) (a) Toon, O. B.; Ackerman, T. P. *Appl. Opt.* **1981**, *20*, 3657. (b) Kurtz, V.; Salib, S. *J. Imaging Sci. Technol.* **1993**, *37*, 43. (c) Bohren, C. F.; Huffman, D. R. *Absorption and Scattering of Light by Smll Particles*; Wiley: New York, 1983.

(17) Kittel, C. *Introduction to Solid State Physics*, 2nd ed.; Wiley: New York, 1956.

(18) (a) Teranishi, T.; Kiyokawa, I.; Miyake, M. *Adv. Mater.* **1998**, *10*, 596. (b) Han, M. Y.; Quek, C. H. *Langmuir* **2000**, *16*, 362.

(19) (a) Pastoriza-Santos, I.; Liz-Marzan, L. M. *Langmuir* **2002**, *18*, 2888. (b) Yin, B. S.; Ma, H. Y.; Wang, S. Y.; Chen, S. H. *J. Phys. Chem. B* **2003**, *107*, 8898. (c) Huang, H. H.; Ni, X. P.; Loy, G. L.; Chew, C. H.; Tan, K. L.; Loh, F. C.; Deng, J. F.; Xu, G. Q. *Langmuir* **1996**, *12*, 909.

(20) (a) Teranishi, T.; Miyake, M. *Chem. Mater.* **1998**, *10*, 594. (b) Narayanan, R.; El-Sayed, M. A. *J. Am. Chem. Soc.* **2003**, *125*, 8340.

(21) (a) Teranishi, T.; Hosoe, M.; Tanaka, T.; Miyake, M. J *Phys. Chem. B* **1999**, *103*, 1818. (b) Chen, W. X.; Lee, J. Y.; Liu, Z. L. *Chem. Commun. (Cambridge, U.K.)* **2002**, *21*, 2588.

(22) Wang, Y. W.; Hong, B. H.; Lee, J. Y.; Kim, J.-S.; Kim, G. H.; Kim, K. S. *J. Phys. Chem. B* **2004**, *108*, 16723.

(23) Diaz, E.; Valenciano, R. B.; Katime, I. A. *J. Appl. Polym. Sci.* **2004**, *93*, 1512.

(24) Hao, H.; Lian, T. Q. *Chem. Mater.* **2000**, *12*, 3392.

(25) Zhang, Z. T.; Zhao, B.; Hu, L. M. *J. Solid State Chem.* **1996**, *121*, 105.

(26) Perenboom, J. A. A.; Wyder, P.; Meier, F. *Phys. Rep.* **1981**, *78*, 173.

(27) Alvarez, M. M.; Khoury, J. T.; Schaaff, T. G.; Shafigullin, M. N.; Vezmar, I.; Whetten, R. L. *J. Phys. Chem. B* **1997**, *101*, 3706.

(28) Weare, W. W.; Reed, S. M.; Warner, M. G.; Hutchison, J. E. *J. Am. Chem. Soc.* **2000**, *122*, 12890.